

UC Berkeley

UC Berkeley Previously Published Works

Title

Optimizing COVID-19 control with asymptomatic surveillance testing in a university environment.

Permalink

<https://escholarship.org/uc/item/85t8c741>

Authors

Brook, Cara E
Northrup, Graham R
Ehrenberg, Alexander J
[et al.](#)

Publication Date

2021-12-01

DOI

10.1016/j.epidem.2021.100527

Peer reviewed



Since January 2020 Elsevier has created a COVID-19 resource centre with free information in English and Mandarin on the novel coronavirus COVID-19. The COVID-19 resource centre is hosted on Elsevier Connect, the company's public news and information website.

Elsevier hereby grants permission to make all its COVID-19-related research that is available on the COVID-19 resource centre - including this research content - immediately available in PubMed Central and other publicly funded repositories, such as the WHO COVID database with rights for unrestricted research re-use and analyses in any form or by any means with acknowledgement of the original source. These permissions are granted for free by Elsevier for as long as the COVID-19 resource centre remains active.



Optimizing COVID-19 control with asymptomatic surveillance testing in a university environment

Cara E. Brook^{a,b,*}, Graham R. Northrup^c, Alexander J. Ehrenberg^{a,d,e,f}, the IGI SARS-CoV-2 Testing Consortium^d, Jennifer A. Doudna^{d,g,h,i,j,l,m,n}, Mike Boots^{a,k}

^a Department of Integrative Biology, University of California, Berkeley, United States

^b Department of Ecology and Evolution, University of Chicago, United States

^c Center for Computational Biology, College of Engineering, University of California, Berkeley, United States

^d Innovative Genomics Institute, University of California, Berkeley, United States

^e Helen Wills Neuroscience Institute, University of California, Berkeley, United States

^f Memory and Aging Center, Weill Institute for Neurosciences, University of California, San Francisco, United States

^g Department of Molecular and Cell Biology, University of California, Berkeley, United States

^h College of Chemistry, University of California, Berkeley, United States

ⁱ J. David Gladstone Institutes, San Francisco, CA, United States

^j Howard Hughes Medical Institute, University of California, Berkeley, United States

^k Department of Biosciences, University of Exeter, Penryn, UK

^l California Institute for Quantitative Biosciences (QB3), University of California, Berkeley, Berkeley, CA, USA

^m MBIB Division, Lawrence Berkeley National Laboratory, Berkeley, Berkeley, CA, USA

ⁿ Gladstone-UCSF Institute of Genomic Immunology, San Francisco, CA, USA

ARTICLE INFO

Keywords:

COVID-19
Asymptomatic surveillance testing
Branching process model
University control

ABSTRACT

The high proportion of transmission events derived from asymptomatic or presymptomatic infections make SARS-CoV-2, the causative agent in COVID-19, difficult to control through the traditional non-pharmaceutical interventions (NPIs) of symptom-based isolation and contact tracing. As a consequence, many US universities developed asymptomatic surveillance testing labs, to augment NPIs and control outbreaks on campus throughout the 2020–2021 academic year (AY); several of those labs continue to support asymptomatic surveillance efforts on campus in AY2021–2022. At the height of the pandemic, we built a stochastic branching process model of COVID-19 dynamics at UC Berkeley to advise optimal control strategies in a university environment. Our model combines behavioral interventions in the form of group size limits to deter superspreading, symptom-based isolation, and contact tracing, with asymptomatic surveillance testing. We found that behavioral interventions offer a cost-effective means of epidemic control: group size limits of six or fewer greatly reduce superspreading, and rapid isolation of symptomatic infections can halt rising epidemics, depending on the frequency of asymptomatic transmission in the population. Surveillance testing can overcome uncertainty surrounding asymptomatic infections, with the most effective approaches prioritizing frequent testing with rapid turnaround time to isolation over test sensitivity. Importantly, contact tracing amplifies population-level impacts of all infection isolations, making even delayed interventions effective. Combination of behavior-based NPIs and asymptomatic surveillance also reduces variation in daily case counts to produce more predictable epidemics. Furthermore, targeted, intensive testing of a minority of high transmission risk individuals can effectively control the COVID-19 epidemic for the surrounding population. Even in some highly vaccinated university settings in AY2021–2022, asymptomatic surveillance testing offers an effective means of identifying breakthrough infections, halting onward transmission, and reducing total caseload. We offer this blueprint and easy-to-implement modeling tool to other academic or professional communities navigating optimal return-to-work strategies.

* Correspondence to: 1101 East 57th Street, Chicago, IL 60637, United States.

E-mail address: cbrook@uchicago.edu (C.E. Brook).

<https://doi.org/10.1016/j.epidem.2021.100527>

Received 31 January 2021; Received in revised form 26 October 2021; Accepted 12 November 2021

Available online 15 November 2021

1755-4365/© 2021 The Author(s).

Published by Elsevier B.V. This is an open access article under the CC BY-NC-ND license

(<http://creativecommons.org/licenses/by-nc-nd/4.0/>).

1. Introduction

Non-pharmaceutical interventions (NPIs) to control the spread of infectious diseases vary in efficacy depending on the natural history of pathogen that is targeted (Fraser et al., 2004). Highly transmissible pathogens and pathogens for which the majority of onward transmission events take place prior to the onset of symptoms are notoriously difficult to control with standard public health approaches, such as isolation of symptomatic individuals and contact tracing (Fraser et al., 2004). SARS-CoV-2, the causative agent in COVID-19, is a clear example of one of these difficult-to-control pathogens (Ferretti et al., 2020). While the first SARS-CoV was effectively contained via the isolation of symptomatic individuals following emergence in 2002 (Petersen et al., 2020), at the time of this article's revision, SARS-CoV-2 remains an ongoing public health menace that has infected more than 240 million people worldwide (WHO, 2020). Though the two coronaviruses are epidemiologically comparable in their original basic reproduction numbers (R_0) (Petersen et al., 2020), SARS-CoV-2 has evaded control efforts largely because the majority of virus transmission events occur prior to the onset of clinical symptoms in infected persons (Ferretti et al., 2020)—in stark contrast to infections with the first SARS-CoV (Petersen et al., 2020). Indeed, in many cases, SARS-CoV-2-infected individuals never experience symptoms at all (Oran and Topol, 2020; Mizumoto et al., 2020; Nishiura et al., 2020; Treibel et al., 2020) but, nonetheless, remain capable of transmitting the infection to others (Emery et al., 2020; Gandhi et al., 2020; Boyles, 2020; Kam et al., 2020; Bai et al., 2020). Due to the challenges associated with asymptomatic and presymptomatic transmission (Gandhi et al., 2020), surveillance testing of asymptomatic individuals has played an important role in COVID-19 epidemic control (Larremore et al., 2021; Bergstrom et al., 2020; Paltiel et al., 2020). Asymptomatic surveillance testing is always valuable for research purposes, but its efficacy as a public health intervention will depend on both the epidemiology of the focal infection and the characteristics of the testing regime. Here, we explore the effects of both behavior-based NPIs and asymptomatic surveillance testing on COVID-19 control in a university environment.

In year two of the COVID-19 pandemic, the United States still leads the globe with over 46 million reported cases of COVID-19 (WHO, 2020), and universities across the nation continue to struggle to control epidemics in their campus communities (Hubler and Hartocollis, 2020). To combat this challenge in AY2020–2021, colleges adopted a variety of largely independent COVID-19 control tactics, ranging from entirely virtual formats to a mix of in-person and remote learning, paired with strict behavioral regulations, and—in some cases—in-house asymptomatic surveillance testing (Richtel, 2020). In AY2021–2022, asymptomatic surveillance testing continues to play a key role in expanded plans for university reopening (Richtel, 2020; Nietzel, 2020), even on some campuses which also mandate vaccination (Vaziri and Asimov, 2021). In March 2020, shortly after the World Health Organization declared COVID-19 to be a global pandemic (Ghebreyesus, 2020), the University of California, Berkeley, launched its own pop-up SARS-CoV-2 testing lab in the Innovative Genomics Institute (IGI) (Amen et al., 2020) with the aim of providing COVID diagnostic services to the UC Berkeley community and underserved populations in the surrounding East Bay region. Though the IGI RT-qPCR-based pipeline was initially developed to service clinical, symptomatic nasopharyngeal and oropharyngeal swab samples (Amen et al., 2020), the IGI subsequently inaugurated an asymptomatic surveillance testing program for the UC Berkeley community (Ehrenberg et al., 2021), through which—at the time of this revision—over 60,000 faculty, students, and staff in the UC Berkeley community have since been serviced with over 440,000 tests and counting (UC Berkeley COVID-19 Dashboard, 2020). From June 2020–May 2021, weekly asymptomatic surveillance testing was mandatory for any UC Berkeley community member working on campus; testing requirements were relaxed in May 2021 for those providing proof of vaccination.

Here we developed a stochastic, agent-based branching process model of COVID-19 spread in a university environment to advise UC Berkeley on best-practice approaches for asymptomatic surveillance testing in our community and to offer guidelines for optimal control in university settings more broadly. Previous modeling efforts have used similar approaches to advocate for more frequent testing with more rapid turnaround times at the expense of heightened test sensitivity (Larremore et al., 2021; Bergstrom et al., 2020) or to weigh the cost-effectiveness of various testing regimes against symptom-based screening in closed university or professional environments (Paltiel et al., 2020). Our model is unique in combining both behavioral interventions with optimal testing design in a real-world setting, offering important insights into efficient mechanisms of epidemic control and an effective tool to optimize control strategies.

2. Materials and methods

Our model takes the form of a stochastic branching process model, in which a subset population of exposed individuals (0.5%, derived from the mean percentage of positive tests in our UC Berkeley community (UC Berkeley COVID-19 Dashboard, 2020)) is introduced into a hypothetical 20,000 person community that approximates our university campus utilization goals from spring 2021. With each timestep, the disease parameters for each infected case are drawn stochastically from distributions representing the natural history of the SARS-CoV-2 virus, paired with realistic estimates of the timeline of corresponding public health interventions (Ferretti et al., 2020; Paltiel et al., 2020; Peak et al., 2020) (Fig. 1). Our flexible model (Text S1; published here with open-access R-code (Brook et al., 2020)) allows for the introduction of NPIs for COVID-19 control in four different forms: (1) group size limits, (2) symptom-based isolations, (3) asymptomatic surveillance testing isolations, and (4) contact tracing isolations that follow after cases are identified through screening from symptomatic or asymptomatic surveillance testing (Table 1). Because we focused our efforts on optimal asymptomatic surveillance testing regimes, we did not explicitly model other NPIs, such as social distancing and mask wearing; however, the effects of these behaviors were captured in our representation of R_E -effective (hereafter, R_E) for both within-campus and out-of-campus transmission. Since vaccination against SARS-CoV-2 became widely available during the review process of our article (including a vaccine mandate across the University of California school system (R. of the U. of California, UC issues final COVID-19 vaccination policy, Ucnct., 2021)), we updated our original model to allow for flexible starting conditions that include a variable proportion of vaccinated individuals in a specific university setting. We allowed a randomly selected 5% of vaccinated individuals to become infected and infectious as “breakthrough cases” (consistent with published estimates of vaccine efficacy for the Pfizer-BioNTech mRNA vaccine with the most widespread uptake in the US (Polack et al., 2020)). For simplicity, we assumed that all infectious individuals were equally transmissible, regardless of vaccination status (though see ‘Discussion’ for future research objectives). After experiencing infection, we further assumed that all individuals became recovered and immune for the remaining duration of our simulations, as our focal timescale of interest (the academic semester) is shorter than most projections of the duration of immunity to SARS-CoV-2 (Kissler et al., 2020; Saad-Roy et al., 2020).

R_E is the product of the pathogen basic reproduction number (R_0) and the proportion of the population that is susceptible to disease. R_E is thus a dynamic value which corresponds to the number of new infections caused by a single infection at a given timepoint within a specified community. We computed an independent R_E for each infectious person in our population as a combined result of both heterogeneity in individual infectiousness and heterogeneity in individual contact events that could result in transmission. To determine R_E , we first drew a value of potential cases for each infectious individual from the SARS-CoV-2 negative binomial distribution for R_0 , estimated to have

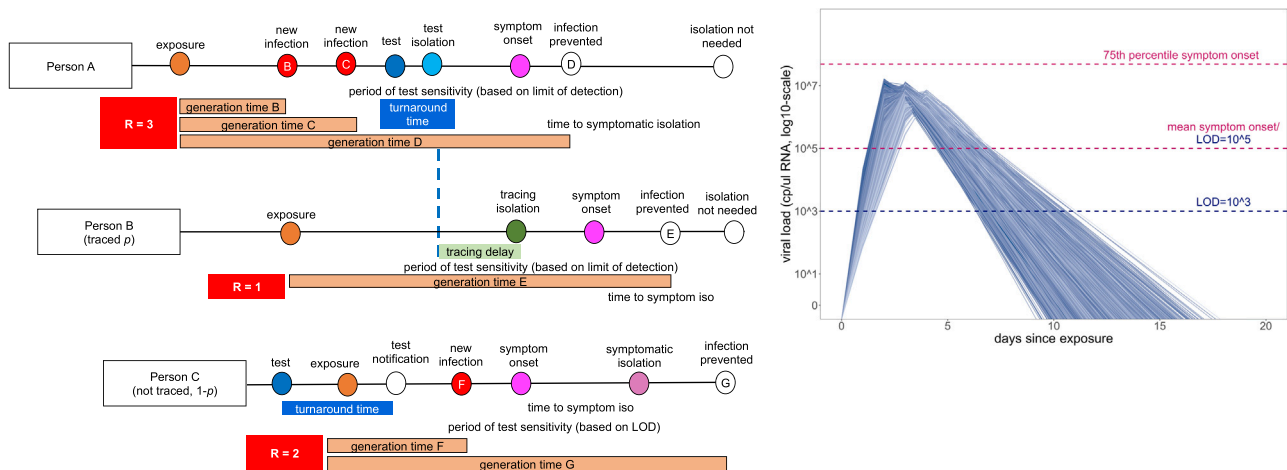


Fig. 1. Conceptual schematic of branching process model of SARS-CoV-2 dynamics. Person A is isolated through testing after exposing Person B and Person C. Person B is then isolated through contact tracing, while Person C is not traced but is nonetheless ultimately isolated through symptomatic surveillance. A viral titer trajectory (right) is derived from a within-host viral kinetics model (Text S2)—independent trajectories from 20,000 randomly-selected individuals are shown here to highlight the range of possible variation. The 25th and 75th titer threshold percentile for the onset of symptoms are depicted in pink, such that 32% of individuals modeled in our simulations did not present symptoms. Schematic is adapted in concept from [Hellewell et al. \(2020\)](#).

a mean value of 2.5 and a dispersion parameter (k) of 0.10 ([Endo et al., 2020](#)); in later analyses incorporating highly vaccinated university settings reflective of the reality of AY2021–2022, we shifted the mean to a value of 6 to better approximate the dynamics of highly transmissible variants of concern (e.g. the Delta variant) ([Liu and Rocklöv, 2021](#)). Though representation of R_E in log-normal vs. negative binomial form will not change the average number of cases generated per epidemic, the negative binomial distribution replicates the dynamics of super-spreading events, which are known to play an important role in SARS-CoV-2 dynamics ([Jumar et al., 2020](#); [Althouse et al., 2020](#); [Hébert-Dufresne et al., 2020](#); [Liu et al., 2020](#); [Adam et al., 2559](#); [Kain et al., 2020](#)). Indeed, there is strong direct empirical evidence that COVID-19 epidemiology exhibits a negative binomial R_E across multiple systems ([Adam et al., 2559](#); [Laxminarayan et al., 2020](#); [Lau et al., 2020](#); [Goyal et al., 2020](#)); as few as 10% of infectious individuals may be responsible for 80% of onward SARS-CoV-2 transmissions ([Nielsen and Sneppen, 2020](#)).

After drawing potential cases for each infectious individual, we next hypothesized that most university students would interact predominantly with other students vs. people from the surrounding community and, thus, modeled only a minority (10%) of possible onward transmissions as lost to the external community (e.g. an infectious UC Berkeley community member infects someone outside the UC Berkeley community), though see ‘Results’ for discussion of sensitivity analysis of this assumption.

Next, we assumed that social distancing, masking, and behavioral modifications in our community would modulate dynamics such that some of the remaining 90% (or 50% in sensitivity analyses) of the original R_0 -derived potential infections do not take place. Because we were specifically interested in advising UC Berkeley on group size limits for gatherings, we then drew a number of possible onward transmission events for each infectious individual from a simple Poisson distribution with $\lambda = 3$, signifying the average number of possible encounters (i.e. cross-household dining, shared car rides, indoor meetings, etc.) per person that could result in transmission. We then use published estimates of the generation time of onward transmission events for SARS-CoV-2 infection ([Ferretti et al., 2020](#)) to draw event times for these encounters and distributed each infectious person’s original number of R_0 -derived potential cases among these events at random. This ensured that multiple transmissions were possible at a single event; the most extreme superspreading events occur when persons with

heterogeneously high infectiousness draw a large number of potential cases, which are concentrated within a relatively small number of discrete transmission events. When we imposed group size limit NPIs in our model, we truncated case numbers for each event at the intervention limit.

For each infectious individual, we additionally generated an independent virus trajectory, using a within-host viral kinetics model for SARS-CoV-2 upper respiratory tract infections, structured after the classic target cell model ([Perelson, 2002](#); [Ho et al., 1995](#); [Nowak and May, 2000](#); [Ke et al., 2020](#)) (Text S2). From each independent virus trajectory, we inferred a time-varying transmissibility, modeled as a Michaelis-Menten-like function of viral load ([Ke et al., 2020](#)). We fixed the within-host viral kinetics model constant, θ , at a value that allowed for a $\sim 50\%$ probability of infection occurring per transmissible contact event at an infectious individual’s peak viral load ([Ke et al., 2020](#)). Because all possible onward transmissions were assigned an event generation time, we next evaluated the viral load of the infectious person at the time of each potential transmission to determine whether or not it actually occurred. By these metrics, our original R_0 -derived possible cases were halved, such that R_E , the number of average onward infections caused by a single infectious person in the UC Berkeley community, was reduced to just over one ($R_E = 1.05$), or just under three ($R_E = 2.94$) in the case of Delta variant simulations, consistent with published estimates of Bay Area R_E and initial asymptomatic test results in our community from the first year of the pandemic ([UC Berkeley COVID-19 Dashboard, n.d.](#); [Schwab et al., n.d.](#)). The majority of modeled transmission events occurred when the infectious host had higher viral titers, thus biasing new case generations towards earlier timesteps in an individual’s infection trajectory, often occurring prior to the onset of symptoms as is realistic for COVID-19 ([Peak et al., 2020](#)) (Fig. 1).

In addition to modulating the probability of onward transmission events, each infectious individual’s virus trajectory additionally allowed us to compute a timing of symptom onset, which corresponded to the timepoint at which an individual’s virus trajectory crossed some threshold value for presentation of symptoms. We drew each threshold randomly from a log-normal distribution with a mean of 10^5 virus copies per μl of RNA; by these metrics, roughly 32% of our modeled population presented as asymptomatic, in keeping with published estimates for SARS-CoV-2 ([Mizumoto et al., 2020](#); [Nishiura et al., 2020](#)). Using each infectious individual’s viral load trajectory, we were next able to

Table 1
Parameter ranges and interventions included in model.

Parameter	Values investigated	References ^a
Basic epidemiology		
Population size	• 20,000	–
Number initially infected	• 100	–
Possible cases per infectious individual (R_0), prior to environmental corrections	<ul style="list-style-type: none"> • Negative binomial distribution (main text): mean = 2.5; $k = 0.10$ • Lognormal distribution (Fig. S2): mean = 2.5; sd = 0.10 • Negative binomial distribution, Delta (Fig. S7, S8): mean = 2.5; $k = 0.10$. 	(Endo et al., 2020; Liu and Rocklöv, 2021)
Transmission events per infectious individual	• Poisson distribution: $\lambda = 3$	–
Virus generation time	• Weibull distribution: $k = 2.826$; $\lambda = 5.665$	(Ferretti et al., 2020)
Proportion of transmissions maintained within the UCB community	<ul style="list-style-type: none"> • 90% (main text) • 50% (Fig. S5) 	–
Population proportion vaccinated	<ul style="list-style-type: none"> • 0% (main text) • 97.7% (Fig. S7) • 60% (Fig. S8) 	(UC Berkeley COVID-19 Dashboard, n.d.; University of Alabama System COVID-19 Dashboard, n.d.)
Proportion of vaccinated individuals experiencing breakthrough cases	<ul style="list-style-type: none"> • 0% (main text) • 5% (Fig. S7, S8) 	(Polack et al., 2020)
Threshold viral titer for symptom onset	<ul style="list-style-type: none"> • Lognormal distribution: mean = 10^5 viral cp/μ RNA; sd = 10^4 viral cp/μ (main text; yields ~30% asymptomatic infections) • Lognormal distribution: mean = 10^7 viral cp/μ RNA; sd = 10^4 viral cp/μ (Fig. S3; yields ~50% asymptomatic infections) 	(Mizumoto et al., 2020; Nishiura et al., 2020)
Behavior-based NPIs		
Group size limits	• 6, 12, 16, 20, 50, no limit (main text; Fig. S1, S2)	–
Population proportion adhering to group size limits	<ul style="list-style-type: none"> • 90% (main text; Fig. S2) • 50% (Fig. S1) 	–
Lag time to symptomatic isolation	• Normal distribution: mean = 1,2,3,4,5 days; sd = 0.5 days	–
Lag time to contact tracing	• Normal distribution: mean = 1 day; sd = 0.5 days	–
Population proportion participating in contact tracing	<ul style="list-style-type: none"> • 0% (main text) • 90% (Fig. S4) 	–
Testing interventions		
Testing frequency	<ul style="list-style-type: none"> • semi-weekly (2x/week) • weekly • every-two-weeks 	–
Test days per week	<ul style="list-style-type: none"> • 2 (main text) • 5, 7 (Fig. S6) 	–
Testing turnaround time	• Normal distribution: mean = 1,2,3,4,5,10 days; sd = 0.5 days	–
Test limit of detection	• 10^1 , 10^3 , 10^5 viral cp/ μ RNA	(Amen et al., 2020; Vogels et al., 2020; Meyerson et al., 2020; Dao Thi et al., 2020; Bordi et al., 2020; Fiedler et al., 2021)

^a if applicable; otherwise, indicates a parameter investigated in this analysis.

compute a period of test sensitivity, corresponding to the time during which viral load is high enough for detection by the virus test in question, based on the modeled limit of detection. Asymptomatic surveillance testing results in higher “false-negative” test results both very early and very late in infection when viral loads are below the detection limit for the adopted assay (Kucirka et al., 2020) (Fig. 1), though most tests should reliably detect infectious cases with viral titers $> 10^6$ cp/ μ l (Wölfel et al., 2020; Quicke et al., 2020; La Scola et al., 2020). We explored dynamics across a range of published values for test limits of detection: 10^1 , 10^3 , and 10^5 virus copies per μ l of RNA. The IGI’s RT-qPCR-based testing pipeline has a published sensitivity of 1 cp/ μ l (Amen et al., 2020), while the majority of SARS-CoV-2 RT-qPCR tests nationally are reliable above a 10^3 cp/ μ l threshold (Vogels et al., 2020); less-sensitive antigen-based and LAMP assays report detection limits around 10^5 cp/ μ l (Meyerson et al., 2020; Dao Thi et al., 2020). Some commercially-available COVID-19 test kits report detection limits in TCID₅₀/ml, which corresponds to the median tissue culture infectious dose, roughly approximating a threshold for the infectious viral load. Though exact values will vary depending on the virus, cell type, and assay conditions, a 100 TCID₅₀/ml limit of detection for SARS-CoV-2 has been shown to correspond to a viral load detection limit between 10^2 and 10^3 cp/ μ l RNA (Bordi et al., 2020; Fiedler et al., 2021). For reference, the Abbot BinaxNOW™ COVID-19 Ag card reports a limit of detection of 140.6 TCID₅₀/ml (between 10^2 and 10^3 cp/ μ l RNA), while the QuickVue At-Home COVID-19 test reports a limit of detection of 1.91×10^4 TCID₅₀/ml (between 10^4 and 10^5 cp/ μ l RNA).

In addition to within-community transmissions, all individuals in the modeled population were also subjected to a daily hazard (0.25% in standard model runs and 0.60% in Delta variant runs) of becoming infected from an external source, based on published estimates of R_E and COVID-19 prevalence in Alameda County (Schwab et al., n.d.; Chitwood et al., 2020). We report the mean results of 100 stochastic runs of each proposed intervention.

3. Results

3.1. Comparing behavioral NPIs for COVID-19 control

We first ran a series of epidemic simulations using a completely mixed population of 20,000 individuals subject to the infection dynamics outlined above to compare and contrast the impacts of our four NPIs on COVID-19 control. We introduced an initial population of 100 infectious individuals (0.5%) at timestep 0 and compared the effects of a single intervention on epidemic trajectories after the first 50 days of simulation. Less intensive or intervention-absent scenarios allowed infectious cases to grow at unimpeded exponential rates, rapidly exhausting our susceptible supply and making it necessary to compare results at a consistent (and early) timepoint in our simulated epidemics.

As a consequence of our representation of R_E in negative binomial form, we first considered the COVID-19 control effectiveness of group size limits on in-person gatherings, which doubled as upper thresholds in transmission capacity (Fig. 2). Assuming that 90% of the modeled population adhered to assumed group size regulations, we found that limiting outdoor gatherings to groups of six or fewer individuals saved a mean of ~7900 cases per 50-day simulation (in a 20,000 person population) and corresponded to an R_E reduction of nearly 0.20 (reducing R_E from 1.05 to subclinical 0.86; Fig. 2; Dataset S1). By contrast, a large group size limit of 50 persons had almost no effect on epidemic dynamics; under published estimates of SARS-CoV-2 negative binomial R_E (Endo et al., 2020), a group size limit of 50 will restrict transmission from only 0.00039% of infectious individuals (Fig. 2). Intriguingly, in sensitivity analyses exploring assumptions of only 50% adherence to group size limits, we witnessed larger caseloads only at group size limits of 16 or fewer individuals (Fig. S1); at group sizes of 20 or more individuals, density limits were so ineffective already that reducing adherence had no power to further undermine the intervention’s

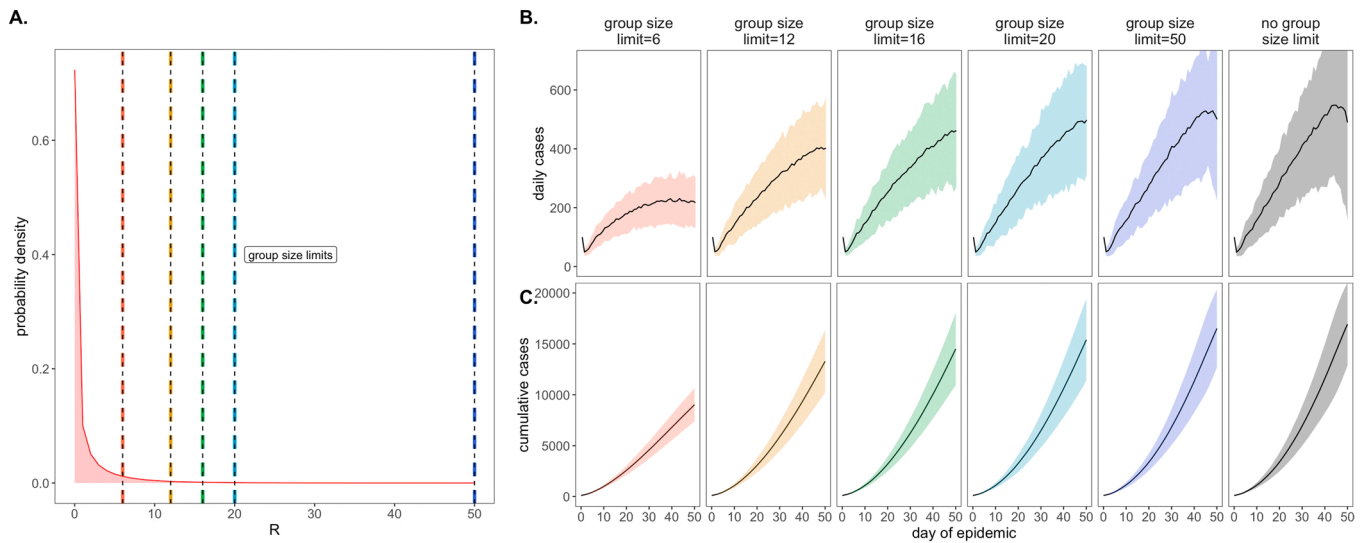


Fig. 2. Effects of group size limits on COVID-19 dynamics., A. Negative binomial R_E distribution with mean = 1.05 and dispersion parameter (k) = 0.10. The colored vertical dashes indicate group size limits that ‘chop the tail’ on the R_E distribution; for 90% of the population, coincident cases allocated to the same transmission event were truncated at the corresponding threshold for each intervention. B. Daily new cases and, C. Cumulative cases, across a 50-day time series with 95% confidence intervals by standard error depicted under corresponding, color-coded group size limits.

impacts. Gains in epidemic control from group size limits resulted from avoidance of superspreading events, an approach that was effective for negative binomial but not log-normal representations of R_E that lack the transmission “tail” characteristic of a superspreader distribution (Kain

et al., 2020) (Fig. S2). Importantly, by avoiding superspreading events, group size limits also reduced variance in daily case counts, yielding more predictable epidemics, which are easier to control through testing and contact tracing (Ferretti et al., 2020; Peak et al., 2020; Hellewell

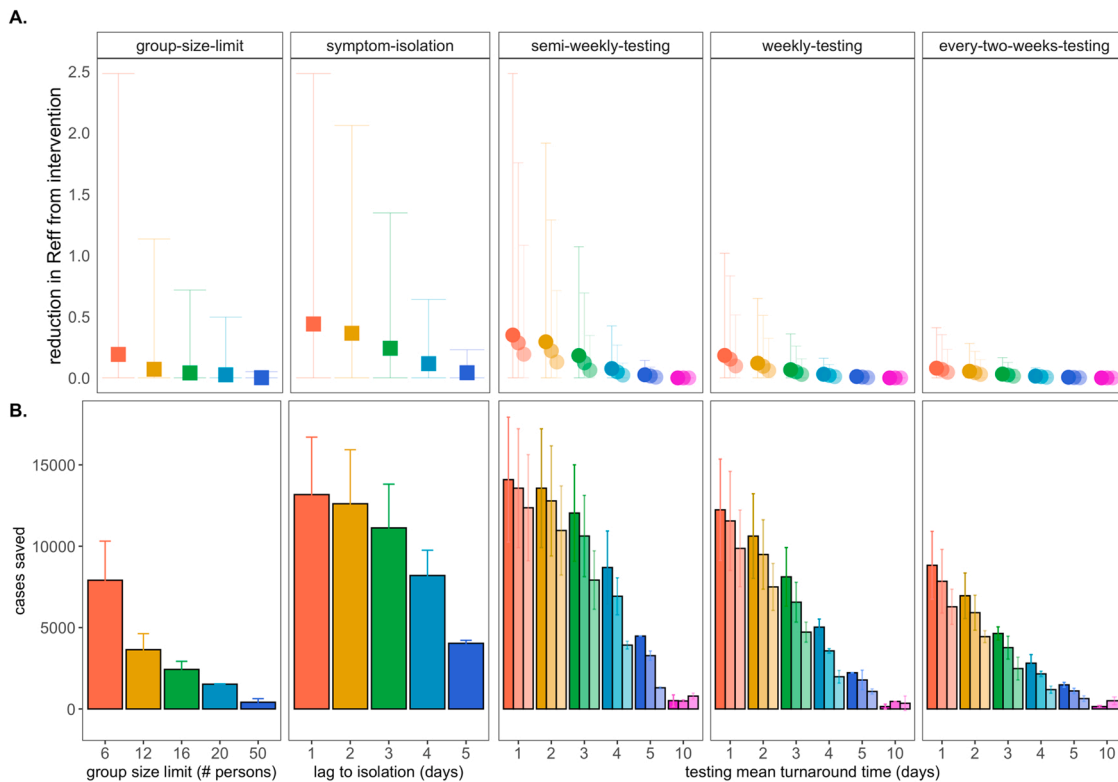


Fig. 3. Impacts of NPIs on COVID-19 control., A. Mean reduction in R_E * and B. cumulative cases saved across 50-day simulated epidemics under assumptions of differing non-pharmacological interventions (NPIs). NPIs are color-coded by threshold number of persons for group-size limits, lag-time for symptom-based isolations, and mean turnaround time from test positivity to isolation of infectious individuals for testing isolations. For testing isolations, shading hue corresponds to test limit of detection with the darkest colors indicating the most sensitive tests with a limit of detection of 10^1 virus copies/ μ l of RNA. Progressively lighter shading corresponds to limits of detection = 10^3 , 10^5 , and 10^7 cp/ μ l. *Note: R_E reduction (panel A) is calculated as the difference in mean R_E in the absence vs. presence of a given NPI. The upper confidence limit (uci) in R_E reduction is calculated as the difference in uci R_E in the absence vs. presence of NPI. In our model, mean R_E in the absence of NPI equals 1.05 and uci R_E in the absence of NPI equals 8.6.

et al., 2020). Over the July 4, 2020 weekend, asymptomatic surveillance testing resources in our UC Berkeley community were overwhelmed and containment efforts challenged after a single superspreading event on campus (U.B. Public Affairs, 2020).

We next investigated the impacts of variation in lag time to self-isolation post-symptom onset for the just under 70% of individuals likely to present with COVID-19 symptoms in our modeled population (Fig. 3). At UC Berkeley, all essential students, faculty, and staff must complete a digital ‘Daily Symptom Screener’ before being cleared to work on campus; here, we effectively modeled the delay post-initial symptom onset to the time at which each individual recognizes symptoms sufficiently to report to the Screener and isolate. For each infected individual in our population, we drew a symptom-based isolation lag from a log-normal distribution centered on a mean of one to five days, assuming the entire population to be compliant with the selected lag.

By these metrics, a rapid, one day lag in symptom-based isolation was the fourth-most effective intervention in our study, with a mean of more than 13,100 cases saved in a 50-day simulation (again, in a 20,000 person population), corresponding to an R_E reduction of 0.67, from 1 to 0.38 (Dataset S1). Longer lag times to isolation produced less dramatic results, but even an average five-day lag to isolation post-symptom onset nonetheless yielded more than 4,000 cases saved and reduced R_E by a mean of 0.06. The efficacy of symptom-based isolation decreased at higher virus titer thresholds for symptom onset, corresponding to a higher asymptomatic proportion (~50%) of the population (Fig. S3); some empirical findings suggest that these higher titer thresholds for symptom onset may more accurately reflect COVID-19 epidemiology (Poletti et al., 2020). Because both group size limits and daily screening surveys to facilitate symptom-based isolation can be implemented without expending substantial resources, we advocate for these two approaches as particularly cost-effective COVID-19 control strategies for all university and small community environments—especially those lacking an on-site asymptomatic surveillance testing lab.

4. Comparing asymptomatic surveillance testing for COVID-19 control

Our primary motivation in developing this model was to advise UC Berkeley on best-practices for asymptomatic surveillance testing. As such, we focused efforts on determining the most effective use of testing resources by comparing asymptomatic surveillance testing across a range of approaches that varied test frequency, test turnaround time (the time from which the test was administered to the timing of positive case isolation), and test sensitivity (based on the limit of detection).

We compared all permutations of asymptomatic surveillance testing, varying test frequency across semi-weekly, weekly, and every-two-week regimes, investigating turnaround time across delays of one to five and ten days, and exploring limits of detection of 10^1 , 10^3 , and 10^5 virus copies per μl of RNA. These test frequency regimes reflect those considered by UC Berkeley administrators throughout the pandemic: from August-December 2020 and January-April 2021, UC Berkeley undergraduates residing in university residence halls were subject to compulsory semi-weekly asymptomatic surveillance testing, while all other campus community members were permitted to take part in voluntary testing with a recommended weekly or every-two-week frequency. After vaccines became widespread (and eventually mandated), testing requirements for vaccinated undergraduates in residence halls were reduced to once a month. Turnaround time values in our model reflect the reality in range of testing turnaround times from in-house university labs like that at UC Berkeley to institutions forced to out-source testing to commercial suppliers (Wu, 2020), and limits of detection span the range in sensitivity of available SARS-CoV-2 tests (Amen et al., 2020; Vogels et al., 2020; Meyerson et al., 2020; Dao Thi et al., 2020).

Across testing regimes broadly, we found test frequency, followed by turnaround time, to be the most effective NPIs, with limit of detection

exerting substantially less influence on epidemic dynamics, consistent with findings published elsewhere (Larremore et al., 2021; Bergstrom et al., 2020). The top three most effective NPIs in our study corresponded to semi-weekly testing regimes with one- and two-day turnaround times across 10^1 and 10^3 cp/ μl limits of detection. These three scenarios yielded mean cases saved ranging from just over 14,000 to just over 13,500 in the first 50 days of simulation and produced an R_E reduction capacity between 0.97 and 0.80 (Fig. 3; Dataset S1). Halving test frequency to a weekly regimen, under assumptions of turnaround time = 1 day and limit of detection = 10^1 , resulted in a nearly 48% decrease in the NPI’s R_E reduction capacity. By comparison, a single extra day lag from one to two-day turnaround time under semi-weekly testing conditions at limit of detection = 10^1 cp/ μl yielded a modest 16% decrease in R_E reduction capacity. However, longer delays in turnaround time of up to ten days or more—not unusual in the early stages of the COVID-19 pandemic (Wu, 2020)—were not significantly different from scenarios in which no intervention was applied at all. This outcome results from the rapid generation time of SARS-CoV-2 (Ferretti et al., 2020); most infectious individuals will have already completed the majority of subsequent transmissions by the time a testing isolation with a 10-day turnaround time is implemented. Nonetheless, encouragingly, reducing test sensitivity from 10^1 to 10^3 under a semi-weekly, turnaround time = 1 day regime decreased R_E reduction capacity by only 18%, offering support to advocates for more frequent but less sensitive tests (Meyer and Madrigal, 2020) but also highlighting the added benefit incurred when university testing labs, like that at UC Berkeley, are able to provide both frequent and sensitive PCR-based testing.

Addition of a contact tracing intervention, in which 90% of infectious contacts were traced and isolated within a day of the source host isolation, to NPI scenarios already featuring either symptom-based or asymptomatic surveillance testing isolation enhanced each intervention’s capacity for epidemic control (Fig. S4). Of note, contact tracing boosted performance of some of the poorest performing testing interventions, such that even those previously ineffective asymptomatic surveillance regimens with 10-day turnaround time nonetheless averted cases and significantly reduced R_E when infectious contacts could be isolated. For a semi-weekly testing regime at limit of detection = 10^1 cp/ μl and turnaround time = 10 days, the addition of contact tracing increased mean cases saved from ~510 to > 8600 and increased R_E reduction capacity from 0.000080 to 0.27 (Dataset S2).

5. Optimizing combined NPIs for COVID-19 control

Our modeled simulations suggested that it is possible to achieve largely equivalent gains in COVID-19 control from NPIs in the form of group size limits, symptom-based isolations, and asymptomatic surveillance testing isolations—though gains from symptom-based behavioral isolations were jeopardized under assumptions of a higher proportion of asymptomatic individuals (Fig. S3). Nonetheless, the most effective interventions were realized when behavioral control mechanisms were combined with asymptomatic surveillance testing (Fig. 4). Assuming a one day turnaround time and 10^1 cp/ μl limit of detection, we found that adding (a) contact tracing with 90% adherence and a one-day lag, plus (b) symptom-based isolation with a one-day lag, plus (c) a group size limit of twelve persons to an every-two-week asymptomatic surveillance testing regimen could elevate the R_E reduction capacity from 0.22 to 0.83 and almost double the ~6600 cases saved from the testing intervention alone (Dataset S3). Combining interventions enabled less rigorous testing regimes to rival the effectiveness of semi-weekly asymptomatic surveillance testing without expending additional resources. In addition, combining interventions resulted in less variation in the cumulative case count, as many layers of opportunity for infection isolation helped limit the likelihood of a superspreading event spiraling out of control. Sensitivity analyses indicated that our findings were largely robust to assumptions of exacerbated insularity in

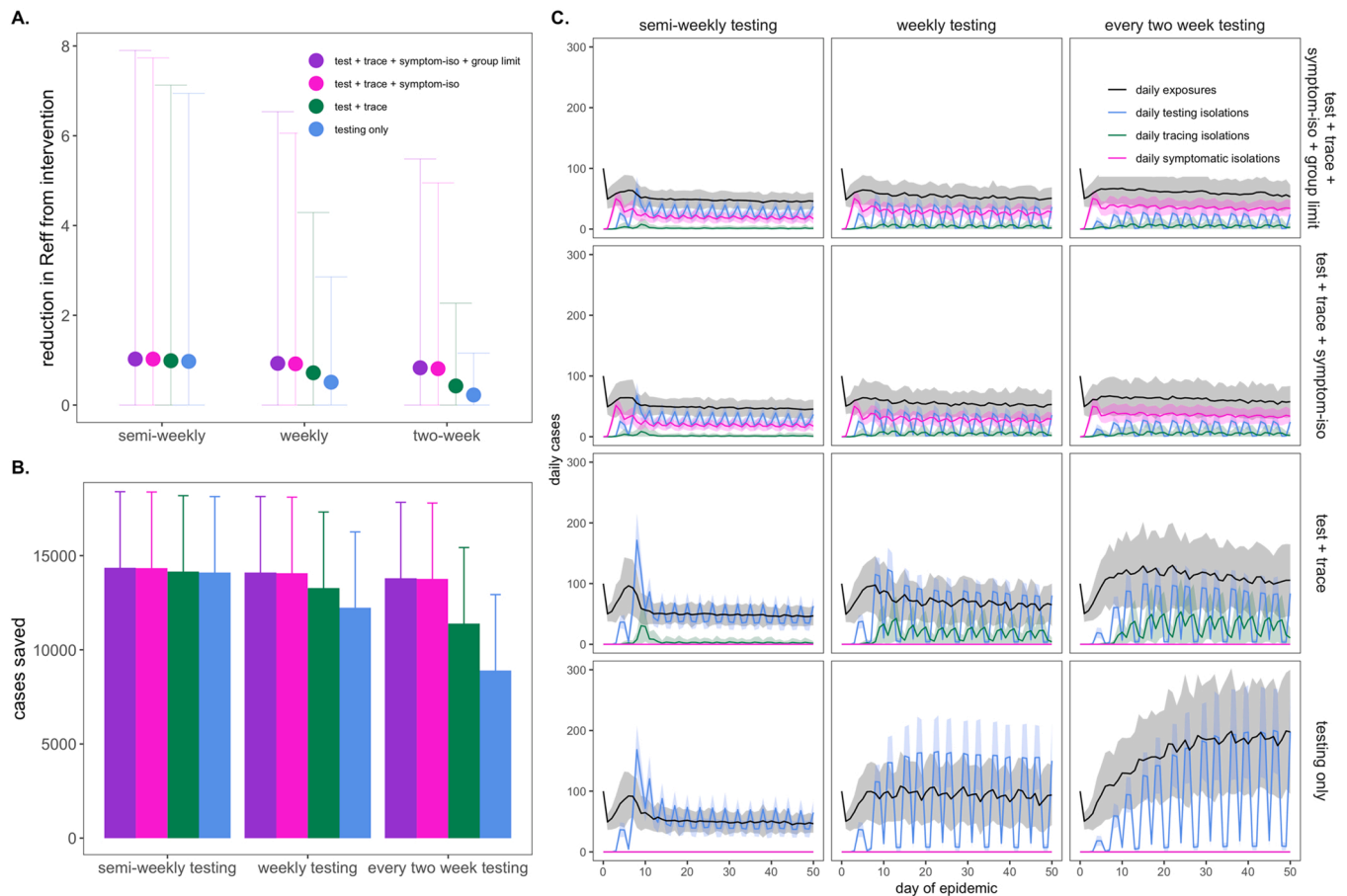


Fig. 4. Combining behavioral and asymptomatic surveillance testing NPIs for COVID-19 control., A. Mean reduction in R_E^* , B. cumulative cases saved, and C. daily case counts for the first 50 days of the epidemic, across regimes of differing testing frequency and a combination of asymptomatic surveillance testing, contact tracing, symptomatic isolation, and group size limit interventions. All scenarios depicted here assumed test turnaround time, symptomatic isolation lags, and contact tracing lags drawn from a log-normal distribution with mean=one day. Limit of detection was fixed at 10^1 and group size limits at 12. Dynamics shown here are from simulations in which testing was limited to two test days per week., *Note: R_E reduction (panel A) is calculated as the difference in mean R_E in the absence vs. presence of a given NPI. The upper confidence limit (uci) in R_E reduction is calculated as the difference in uci R_E in the absence vs. presence of NPI. In our model, mean R_E in the absence of NPI equals 1.05 and uci R_E in the absence of NPI equals 8.6.

university settings (e.g. when only 1% of transmissions were lost to the outside) but that the impacts of combined interventions were reduced under sensitivity analyses exploring a higher proportion (e.g. 50%) of transmissions lost to the external community (Fig. S5), as interventions can only be applied within the closed campus. These findings highlight the vulnerability of any community public health control measure to disease introductions from beyond the sphere of control. On a macro-scale, isolated countries like New Zealand have struggled with this challenge across the course of the COVID-19 pandemic (Geoghegan et al., 2020).

Finally, we also experimented with varying the distribution of days allocated to asymptomatic surveillance testing, without changing the frequency with which each individual was tested. Specifically, we explored semi-weekly, weekly, and every-two-week testing regimens in which tests were administered across two, five, and seven available testing days per week. More broadly distributed test days corresponded to fewer tests per day at a population level but, as with more intervention layers, resulted in less variation in the cumulative total cases because testing isolations more closely tracked daily exposures (Fig. S6).

6. Modeling COVID-19 dynamics in the campus community

We next sought to advise the IGI on asymptomatic surveillance testing strategies explicitly by simulating epidemics in a more realistic, heterogeneous population modeled after the UC Berkeley campus

community in the spring semester of AY2020–2021 (Fig. 5). To this end, we subdivided our 20,000 person university population into a 5,000 person “high transmission risk” cohort and a 15,000 person “low transmission risk” cohort, assuming “high transmission risk” status to correspond to individuals (such as undergraduates), living in high density housing with a majority of contacts (90%) concentrated within the UCB community and “low transmission risk status” to correspond to individuals (such as faculty members or postdoctoral scholars) with only limited contacts (40%) in the UCB community. We imposed a 12-person group size limit (with 90% adherence) on the population as a whole, as recommended by the City of Berkeley Public Health Department in the early months of the pandemic (C. of B.P.H. Officer, 2020), and assumed a one-day average lag in symptom-based isolation for all cohorts. To add additional realism, we enrolled only 50% of each transmission risk group in our modeled asymptomatic surveillance testing program (to mimic adherence—though asymptomatic surveillance testing is compulsory for undergraduates residing in residence halls at UC Berkeley (UC Berkeley COVID-19 Dashboard, n.d.)). We assumed that 95% efficacy in contact tracing (with a mean tracing delay of one day) for those enrolled in our asymptomatic surveillance program but only 50% efficacy for those not enrolled; UC Berkeley has encouraged all community members to enroll in the ‘CA Notify’ digital contact tracing app developed by Apple and Google (U.S.D. Health, CA Notify, 2020). For all testing interventions, we assumed limit of detection = 10^1 cp/μl and turnaround time = 2 days, the average for the IGI asymptomatic

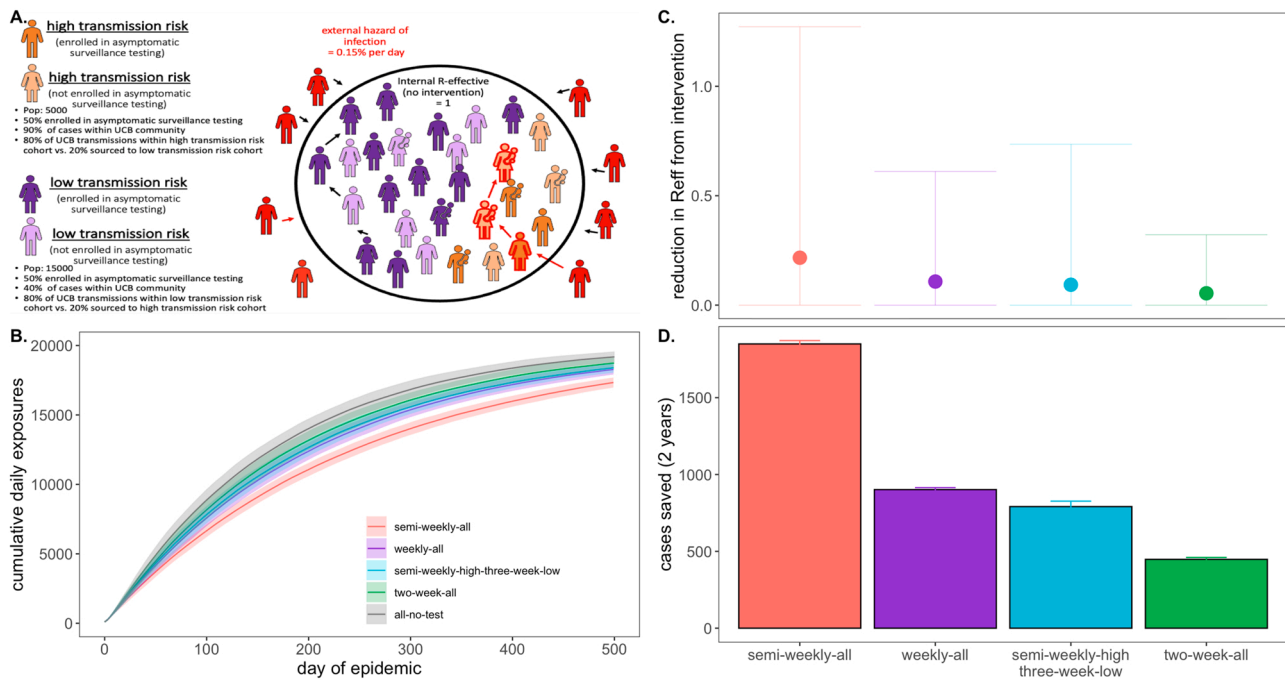


Fig. 5. Targeted testing of high transmission risk cohorts in a heterogeneous population. A. Schematic of transmission risk group cohorts in the heterogeneous model. The population is divided into 5000 “high transmission risk” and 15000 “low transmission risk” individuals, for which, 90% and 40% of the proportion of transmission events take place within the UC Berkeley community, respectively. Of those transmission events within the Berkeley community, the majority (80%) are restricted within the same transmission risk group as the infector, while 20% are sourced to the opposing risk group. Half of each cohort is assumed to be enrolled in asymptomatic surveillance testing and subjected to the differing test frequency regimes depicted in panels B. through D. Panel B. shows the progression of cumulative cases across 730 days of simulation for each testing regime, while panel C. and D. give, respectively, the reduction in R_{E} and the total cases saved achieved by each test regime vs. a no intervention baseline. *Note: R_{E} reduction (panel A) is calculated as the difference in mean R_{E} in the absence vs. presence of a given NPI. The upper confidence limit (uci) in R_{E} reduction is calculated as the difference in uci R_{E} in the absence vs. presence of NPI. In our model, mean R_{E} in the absence of NPI equals 1.05 and uci R_{E} in the absence of NPI equals 8.6.

surveillance testing lab (Amen et al., 2020).

We found that targeted, semi-weekly testing of 50% of individuals in the high transmission risk cohort, paired with every-three-week testing of enrolled individuals in the low transmission risk cohort yielded mean R_{E} reduction and cumulative cases saved on par with that achieved from weekly testing (and better than that achieved from every-two-week testing) of all enrolled individuals in the population at large (Fig. 5). Targeting the highest transmission-risk populations with testing allows practitioners to save valuable resources while simultaneously controlling the epidemic for the entire community. Importantly, while mean R_{E} reduction and cumulative cases were largely comparable between the targeted, semi-weekly testing regiment and the untargeted, weekly regimen, the observed variance in intervention efficacy (Fig. 5C) was substantially greater for the targeted scenario, in which the low transmission risk cohort was only tested once every three weeks. This results from a higher probability that a rare superspreading event could occur in the infrequently monitored low transmission risk cohort, thus reaffirming our previous observation that more frequent asymptomatic surveillance testing regimens result in more predictable—and easier to control—epidemics.

Notably, irrespective of intervention, the diminished transmissibility of the “low transmission risk” population in this heterogeneous model structure greatly reduced epidemic spread in subsequent simulations as compared with those presented previously in the perfectly mixed environment; as a result, we here compared interventions after 500 days of simulation, rather than 50. The heightened realism of our heterogeneous population generated slow-moving epidemics more closely resembling those we witnessed in our university environment across AY2020–2021.

7. Modeling vaccinated environments

During the time in which this article was under review, COVID-19 vaccines became widely available in the US, and the University of California system issued a vaccine mandate for students and staff across all of its campuses, including UC Berkeley (R. of the U. of California, UC issues final COVID-19 vaccination policy, Ucnnet, 2021). Simultaneously, the highly transmissible Delta variant ($R_0 \sim 6$ (Liu and Rocklöv, 2021)) took hold as the most widespread SARS-CoV-2 lineage in the United States (de Rio et al., 2021). To address this new reality, we ran additional simulations of our original, single-population, university testing model, comparing the mosaic of possible interventions exhibited in Fig. 4 under assumptions of $R_0 = 6$ in university settings in which a variable proportion of the student population was vaccinated. Specifically, we compared simulations in a population that was only 60% vaccinated (reflecting the student population of the University of Alabama, Tuscaloosa, a comparably sized public university to UCB but without a vaccine mandate, at the time of writing (University of Alabama System COVID-19 Dashboard, n.d.)) to simulations in a population that was 97.7% vaccinated (reflecting the UC Berkeley undergraduate population at the time of writing (UC Berkeley COVID-19 Dashboard, n.d.)). Over 1000 US universities and colleges have now issued guidelines mandating vaccination (with some exceptions) for on-campus study (Thomason and O’Leary, 2021).

In these new simulations, testing, tracing, symptomatic isolation, and group size limit NPIs continued to have scalable impacts on COVID-19 dynamics within each respective university setting (Fig. S7–S8). Baseline R_{E} under Delta variant assumptions in 60% vaccinated populations without behavior- or testing-based interventions was higher than baseline R_{E} in unvaccinated populations under standard transmission assumptions (1.12 vs. 1.05). Nonetheless, behavior- and testing-

based NPIs easily controlled epidemics in a less susceptible population (Fig. S7). Averted cases were fewer because fewer infections occurred altogether in the partially-vaccinated population. Daily variance in exposure rate narrowed and differences in impact between interventions of variable intensity were less extreme in this more mild epidemic scenario, a pattern even more pronounced in simulations assuming a 97.7% vaccinated population. Under assumptions of near-complete vaccination and Delta transmission, baseline R_E equaled 0.17, and a testing only intervention with an every-two-week frequency was sufficient to avert the majority of onward transmission in the system (Fig. S8). Our findings offer support for some university policies which continue to mandate asymptomatic surveillance testing even for vaccinated individuals (Vaziri and Asimov, 2021), as even modest surveillance efforts still effectively reduced R_E and averted cases in highly vaccinated settings. Our model is structured such that future work could investigate the impact of disparate population sizes, distinct R_0 values reflective of variable contact patterns, and unique vaccination proportions in heterogeneous subgroups within a larger community on longterm epidemic control.

8. Discussion

We built a stochastic branching process model of SARS-CoV-2 spread in a university environment to advise UC Berkeley on best-practice strategies for effective asymptomatic surveillance in our pop-up IGI testing lab—and to offer a model for other institutions attempting to control the COVID-19 epidemic in their communities. While previous work has explored the isolated effects of specific NPIs—including group association limits (Kain et al., 2020), symptomatic isolation (Ferretti et al., 2020; Larremore et al., 2021; Bergstrom et al., 2020; Paltiel et al., 2020; Peak et al., 2020; Hellewell et al., 2020), asymptomatic surveillance testing (Larremore et al., 2021; Bergstrom et al., 2020; Paltiel et al., 2020), and contact tracing (Ferretti et al., 2020; Peak et al., 2020; Hellewell et al., 2020)—on COVID-19 control, ours is unique in investigating these interventions simultaneously in a realistic and easily applicable setting. We offer an easy-to-implement modeling tool that can be applied in other educational and workplace settings to provide NPI recommendations tailored to the COVID-19 epidemiology of a specific environment.

Results from our analysis of behavior-based NPIs support previous work (Ferretti et al., 2020; Larremore et al., 2021; Bergstrom et al., 2020; Paltiel et al., 2020; Peak et al., 2020; Hellewell et al., 2020; Kain et al., 2020) in showing that stringent group size limitations to minimize superspreading events and rapid symptom-based isolations offer an effective means of epidemic control in the absence of asymptomatic surveillance testing resources. However, because of the unique natural history of the SARS-CoV-2 virus, for which the majority of transmission events result from asymptomatic or presymptomatic infections (Ferretti et al., 2020; Hellewell et al., 2020), symptom-based NPIs cannot reduce epidemic spread completely, and small community environments will always remain vulnerable to asymptomatic case importation. Moreover, symptom-based NPIs pose less effective means of epidemic control under scenarios assuming a higher proportion of asymptomatic individuals; empirical evidence suggests that SARS-CoV-2 infection may result in asymptomatic infection in up to nearly 70% of the population in select environments (Poletti et al., 2020). For this reason, our results emphasize the importance of asymptomatic surveillance testing to prevent ongoing epidemics in universities and other small community environments. As more data becomes available on both the proportion of asymptomatic infections and their contributions to SARS-CoV-2 transmission, the relative importance of group size interventions, symptom-based isolation, and asymptomatic surveillance testing in different epidemiological contexts will be possible to determine from our modeling framework.

As with behavioral interventions, our exploration of optimal asymptomatic surveillance testing regimes supports findings that have

been published previously but with some key extensions and critical novel insights. As has been recently highlighted (Larremore et al., 2021; Bergstrom et al., 2020), we find that the most cases are saved under asymptomatic testing regimes that prioritize heightened test frequency and rapid turnaround time over test sensitivity. Importantly, we extend previous work to highlight how more rigorous testing regimes—and those combined with one or more behavioral interventions—greatly reduce variance in daily case counts, leading to more predictable epidemics. We find that the reduction in daily case variation is even more pronounced when test regimes of equivalent frequency are distributed more broadly in time (i.e. tests are offered across more days of the week), thus minimizing the likelihood of compounding transmission chains that may follow upon a superspreading event. Additionally, we demonstrate how a focused stringent testing regime for a subset of “high transmission risk” individuals can effectively control a COVID-19 epidemic for the broader community. Importantly, the extension of our model to heterogeneous community dynamics also paves the way for future work that could explicitly model age-structured mixing patterns and infection probabilities by assigning disparate R_0 values and/or distinct viral load trajectories to different community subgroups. For example, students living in university residence halls may experience a higher daily hazard of infection than older adults in lower density housing (as captured in R_0), and young adult infections may manifest with lower viral load trajectories that are more likely to present as asymptomatic. Similarly, future modeling efforts could explore variable infection probabilities and/or viral titer trajectories in individuals infected after vaccination or otherwise. Taken together, our model shows the utility of a multi-faceted approach to COVID-19 control and offers a flexible tool to aid in prioritization of interventions in different university or workplace settings.

Finally, our paper presents the only COVID-19 asymptomatic surveillance model published to date that combines asymptomatic testing with contact tracing, thus highlighting the compounding gains effected by these two interventions: contact tracing amplifies the control impacts of both symptom-based and asymptomatic surveillance testing-based isolations, such that even intervention scenarios assuming long delays in isolation after symptom onset or slow turnaround-times for test results can nonetheless greatly reduce the transmission capacity of COVID-19. These findings further emphasize the critical role that asymptomatic surveillance testing will continue to play in ongoing efforts to control COVID-19 epidemics in AY 2021–2022. Even limited asymptomatic surveillance testing can offer substantial gains in case reduction for university and workplace settings with high vaccination rates and/or efficient symptomatic isolation and contact tracing programs in place. Our model allows us to prioritize when and where these gains are most likely to be achieved.

Because we do not explicitly model SARS-CoV-2 transmission in a mechanistic, compartmental framework (Anderson et al., 1991; Kermack and McKendrick, 1927), our analysis may overlook some more subtle insights into long-term disease dynamics. More complex analyses of interacting epidemics across larger spatial scales or investigations of the duration of immunity will necessitate implementation of a complete compartmental transmission model. However, our use of a stochastic branching process framework makes our model simple to implement and easily transferrable to other semi-contained small community environments, including a wide range of academic settings and workplaces (Brook et al., 2020). We make this tool available to others interested in exploring the impacts of targeted public health interventions—in particular, asymptomatic surveillance testing regimes—on COVID-19 control in more specific settings. We at the University of California, Berkeley are committed to maintaining the safest campus environment possible for our community, using all intervention tools at our disposal. We advise those in similar positions at other institutions to employ the behavioral interventions outlined here, in concert with effective asymptomatic surveillance testing regimes, to reduce community epidemics of COVID-19 in their own communities.

Funding

This work was supported by the Miller Institute for Basic Research at the University of California, Berkeley [fellowship to CEB], the Branco Weiss Society in Science at ETH Zurich [fellowship to CEB], a DARPA PREEMPT Cooperative Grant [no. D18AC00031], a COVID-19 Rapid Response Research grant from the Innovative Genomics Institute at the University of California, Berkeley, as well as the NIH [no. R01-GM122061-03] and the NSF EEID program [no. 2011109]. The Packard Foundation, the Curci Foundation, the Julia Burke Foundation, The University of California, Berkeley, for their financial support of IGI FAST.

CRedit authorship contribution statement

Cara E. Brook: Conceptualization, Methodology, Software, Validation, Formal analysis, Data curation, Writing – Original draft preparation, Writing – Review & editing, Visualization. **Graham R. Northrup:** Software, Validation, Data curation, Writing – Review & editing. **Alexander J. Ehrenberg:** Conceptualization, Writing – Review & editing, Project administration. **The IGI SARS-CoV-2 Testing Consortium:** Conceptualization, Writing – Review & editing, Resources. **Jennifer A. Doudna:** Conceptualization, Writing – Review & editing, Resources, Supervision. **Mike Boots:** Conceptualization, Writing – Review & editing, Resources, Supervision.

Conflicts of interest

The Regents of the University of California have patents issued and pending for CRISPR technologies on which J.A.D. is an inventor. J.A.D. is a cofounder of Caribou Biosciences, Editas Medicine, Scribe Therapeutics, Intellia Therapeutics and Mammoth Biosciences. J.A.D. is a scientific advisory board member of Vertex, Caribou Biosciences, Intellia Therapeutics, eFFECTOR Therapeutics, Scribe Therapeutics, Mammoth Biosciences, Synthego, Algen Biotechnologies, Felix Biosciences, The Column Group and Inari. J.A.D. is a Director at Johnson & Johnson and Tempus and has research projects sponsored by Biogen, Pfizer, Apple-Tree Partners, and Roche.

Appendix A. Supporting information

Supplementary data associated with this article can be found in the online version at [doi:10.1016/j.epidem.2021.100527](https://doi.org/10.1016/j.epidem.2021.100527).

References

- Adam, D.C., Wu, P., Wong, J.Y., Lau, E.H.Y., Tsang, T.K., Cauchemez, S., Leung, G.M., Cowling, B.J., Cauchemez, S., B.J.C. *, Leung, T., Gabriel, M., 2019. Clustering and superspreading potential of severe acute respiratory syndrome coronavirus 2 (SARS-CoV-2) infections in Hong Kong. *J. Vis. Lang. Comput.* 11, 55. https://www.m-culture.go.th/mculture_th/download/king9/Glossary_about_HM_King_Bhumibol_Aduyadej's_Funeral.pdf.
- Althouse, B.M., Wenger, E.A., Miller, J.C., Scarpino, S.V., Allard, A., Hébert-Dufresne, L., Hu, H., 2020. Stochasticity and heterogeneity in the transmission dynamics of SARS-CoV-2. *ArXiv* 1–10. (<http://arxiv.org/abs/2005.13689>).
- Amen, A.M., Barry, K.W., Brook, C.E., Boyle, J.M., Choo, S., Cornmesser, L.T., Dilworth, D.J., Doudna, J.A., Ehrenberg, A.J., Fedrigo, I., Friedline, S.E., Graham, T. G.W., Green, R., Hamilton, J.R., Hirsch, A., Hochstrasser, M.L., Hockemeyer, D., Krishnappa, N., Lari, A., Li, H., Lin-Shiao, E., Lu, T., Lyons, E.F., Mark, K.G., Martell, L.A., Martins, A.R.O., McDevitt, S.L., Mitchell, P.S., Moehle, E.A., Naca, C., Nandakumar, D., O'Brien, E., Pappas, D.J., Pestal, K., Quach, D.L., Rubin, B.E., Sachdeva, R., Stahl, E.C., Syed, A.M., Tan, I.-L., Tollner, A.L., Tsuchida, C.A., Tsui, C. K., Turkalo, T.K., Urnov, F.D., Warf, M.B., Whitney, O.N., Witkowski, L.B., 2020. Blueprint for a pop-up SARS-CoV-2 testing lab. *Nat. Biotechnol.* 38, 791–797. <https://doi.org/10.1038/s41587-020-0583-3>.
- Anderson, R.M., May, R.M., Boily, M.C., Garnett, G.P., Rowley, J.T., 1991. The spread of HIV-1 in Africa: sexual conflict patterns and the predicted demographic impact of AIDS. *Nature* 352, 581–589.
- Bai, Y., Yao, L., Wei, T., Tian, F., Jin, D.-Y., Chen, L., Wang, M., 2020. Presumed asymptomatic carrier transmission of COVID-19. *J. Am. Med. Assoc.* 382, 1199–1207. <https://doi.org/10.1056/NEJMoa2001316>.
- Bergstrom, T., Bergstrom, C.T., Li, H., 2020. Frequency and accuracy of proactive testing for COVID-19. *MedRxiv*. 2020.09.05.20188839. <https://doi.org/10.1101/2020.09.05.20188839>.
- Bordi, L., Piralla, A., Lalle, E., Giardina, F., Colavita, F., Tallarita, M., Sberna, G., Novazzi, F., Meschi, S., Castilletti, C., Brisci, A., Minnucci, G., Tettamanzi, V., Baldanti, F., Capobianchi, M.R., 2020. Rapid and sensitive detection of SARS-CoV-2 RNA using the SimplexATM COVID-19 direct assay. *J. Clin. Virol.* 128. <https://doi.org/10.1016/j.jcv.2020.104416>.
- Boyles, S., 2020. Covid-19: Asymptomatic transmission fueled nursing home death toll. *Physicians' Wkly.*
- Brook, C.E., Northrup, G.R., Boots, M., 2020. Code for “Optimizing COVID-19 control with asymptomatic surveillance testing in a university environment.” [doi:10.5281/zenodo.4131223](https://doi.org/10.5281/zenodo.4131223).
- C. of B.P.H. Officer, 2020. Order of the Health Officer of the City of Berkeley Imposing Measure Necessary to Control the Spread of COVID-19.
- Chitwood, M.H., Russi, M., Gunasekera, K., Havumaki, J., Pitzer, V.E., Warren, J.L., Weinberger, D.M., Cohen, T., Menzies, N.A., 2020. Menzies3, Bayesian nowcasting with adjustment for delayed and incomplete reporting to estimate COVID-19 infections in the United States. *MedRxiv*. 20 1–6. [doi:10.18907/jjsre.20.7.624.5](https://doi.org/10.18907/jjsre.20.7.624.5).
- Dao Thi, V.L., Herbst, K., Boerner, K., Meurer, M., Kremer, L.P.M., Kirmaier, D., Freistaedter, A., Papagiannidis, D., Galmozzi, C., Stanifer, M.L., Boulant, S., Klein, S., Chlanda, P., Khalid, D., Miranda, I.B., Schnitzler, P., Kräusslich, H.G., Knop, M., Anders, S., 2020. A colorimetric RT-LAMP assay and LAMP-sequencing for detecting SARS-CoV-2 RNA in clinical samples. *Sci. Transl. Med.* 12. <https://doi.org/10.1126/SCITRANSLMED.ABC7075>.
- Ehrenberg, A.J., Moehle, E.A., Brook, C.E., Cate, A.H.D., Witkowski, L.B., Sachdeva, R., Hirsch, A., Barry, K., Hamilton, J.R., Lin-Shiao, E., McDevitt, S., Valentin-Alvarado, L., Letourneau, K.N., Hunter, L., Pestal, K., Frankino, P.A., Murlay, A., Nandakumar, D., Stahl, E.C., Tsuchida, C.A., Gildea, H.K., Murdock, A.G., Hochstrasser, M.L., Bardet, L., Sherry, C., Consortium, T.I.S.-C.-2 T., Harte, A., Nicolette, G., Giannikopoulos, P., Hockemeyer, D., Petersen, M., Urnov, F.D., Ringeisen, B.R., Boots, M., Doudna, J.A., 2021. Launching a saliva-based SARS-CoV-2 surveillance testing program on a university campus. *MedRxiv*. 1–24.
- Emery, J.C., Russell, T.W., Liu, Y., Hellewell, J., Pearson, C.A.B., Knight, G.M., Eggo, R. M., Kucharski, A.J., Funk, S., Flasche, S., Houben, R.M.G.J., Atkins, K.E., Klepac, P., Endo, A., Jarvis, C.I., Davies, N.G., Rees, E.M., Meakin, S.R., Rosello, A., van Zandvoort, K., Munday, J.D., Edmunds, W.J., Jombart, T., Auzenberger, M., Nightingale, E.S., Jit, M., Abbott, S., Simons, D., Bosse, N.I., Leclerc, Q.J., Procter, S. R., Villabona-Arenas, C.J., Tully, D.C., Deol, A.K., Sun, F.Y., Hué, S., Foss, A.M., Prem, K., Medley, G., Gimma, A., Lowe, R., Clifford, S., Quail, H., Diamond, C., Gibbs, H.P., Quilty, B.J., O'reilly, K., 2020. The contribution of asymptomatic SARS-CoV-2 infections to transmission on the Diamond Princess cruise ship. *In: ELife*, 9, pp. 1–68. <https://doi.org/10.7554/ELIFE.58699>.
- Endo, A., Abbott, S., Kucharski, A.J., Funk, S., 2020. Estimating the overdispersion in COVID-19 transmission using outbreak sizes outside China. *Wellcome Open Res.* 5, 67. <https://doi.org/10.12688/wellcomeopenres.15842.3>.
- Ferretti, L., Wymant, C., Kendall, M., Zhao, L., Nurtay, A., Abeler-Dörner, L., Parker, M., Bonsall, D., Fraser, C., 2020. Quantifying SARS-CoV-2 transmission suggests epidemic control with digital contact tracing. *Science* 368, eabb6936. <https://doi.org/10.1126/science.abb6936>.
- Fiedler, M., Holtkamp, C., Dittmer, U., Anastasiou, O.E., 2021. Performance of the LIAISON SARS-CoV-2 antigen assay vs. SARS-CoV-2 RT-PCR. *Pathogens* 10, 1–9. <https://doi.org/10.3390/pathogens10060658>.
- Fraser, C., Riley, S., Anderson, R.M., Ferguson, N.M., 2004. Factors that make an infectious disease outbreak controllable. *Proc. Natl. Acad. Sci. USA* 101, 6146–6151.
- Gandhi, M., Yokoe, D.S., Havlir, D.V., 2020. Asymptomatic transmission, the achilles' heel of current strategies to control COVID-19. *N. Engl. J. Med.* 382, 2158–2160. <https://doi.org/10.1056/NEJMe2009758>.
- Geoghegan, J.L., Ren, X., Storey, M., Hadfield, J., Jelley, L., Jefferies, S., Sherwood, J., Paine, S., Huang, S., Douglas, J., Mendes, F.K., Sporle, A., Baker, M.G., Murdoch, D. R., French, N., Simpson, C.R., Welch, D., Drummond, A.J., Holmes, E.C., Duchêne, S., de Ligt, J., 2020. Genomic epidemiology reveals transmission patterns and dynamics of SARS-CoV-2 in Aotearoa New Zealand. *Nat. Commun.* 11, 1–7. <https://doi.org/10.1038/s41467-020-20235-8>.
- Ghebreyesus, T.A., 2020. WHO director-general's opening remarks at the media briefing on COVID-19. . <https://www.who.int/dg/speeches/detail/who-director-general-s-opening-remarks-at-the-media-briefing-on-covid-19-11-march-2020>.
- Goyal, A., Reeves, D.B., Fabian Cardozo-Ojeda, E., Schiffer, J.T., Mayer, B.T., 2020. Wrong person, place and time: viral load and contact network structure predict SARS-CoV-2 transmission and super-spreading events. *MedRxiv*. 2020.08.07.20169920. ([https://www.medrxiv.org/content/10.1101/2020.08.07.20169920v2.abstract](https://www.medrxiv.org/content/10.1101/2020.08.07.20169920v2%0Ahttps://www.medrxiv.org/content/10.1101/2020.08.07.20169920v2.abstract)).
- Hébert-Dufresne, L., Althouse, B.M., Scarpino, S.V., Allard, A., 2020. Beyond R0: heterogeneity in secondary infections and probabilistic epidemic forecasting. *J. R. Soc. Interface* 17, 20200393. <https://doi.org/10.1101/2020.02.10.20021725>.
- Hellewell, J., Abbott, S., Gimma, A., Bosse, N.I., Jarvis, C.I., Russell, T.W., Munday, J.D., Kucharski, A.J., Edmunds, W.J., Sun, F., Flasche, S., Quilty, B.J., Davies, N., Liu, Y., Clifford, S., Klepac, P., Jit, M., Diamond, C., Gibbs, H., van Zandvoort, K., Funk, S., Eggo, R.M., 2020. Feasibility of controlling COVID-19 outbreaks by isolation of cases and contacts. *Lancet Glob. Heal.* 8, e488–e496. [https://doi.org/10.1016/S2214-109X\(20\)30074-7](https://doi.org/10.1016/S2214-109X(20)30074-7).
- Ho, D.D., Neumann, A.U., Perelson, A.S., Chen, W., Leonard, J.M., Markowitz, M., 1995. Rapid turnover of plasma vireons and CD4 lymphocytes in HIV-1 infection. *Nature* 373, 123–126. <https://doi.org/10.1038/373123a0>.

- Hubler, S., Hartocollis, A., 2020. How Colleges Became the New Covid Hot Spots, New York Times.
- Jumar, S., Jha, S., Rai, S.K., 2020. Significance of super spreader events in COVID-19. *Indian J. Public Health* 64, 139–141.
- Kain, M.P., Childs, M.L., Becker, A.D., Mordecai, E.A., 2020. Chopping the tail: how preventing superspreading can help to maintain COVID-19 control. *MedRxiv Prepr. Serv. Heal. Sci.* doi:10.1101/2020.06.30.20143115.
- Kam, K.Q., Yung, C.F., Cui, L., Lin Tzer Pin, R., Mak, T.M., Maiwald, M., Li, J., Chong, C. Y., Nadua, K., Tan, N.W.H., Thoon, K.C., 2020. A well infant with Coronavirus Disease 2019 (COVID-19) with high viral load. *Clin. Infect. Dis.* ciaa201. <https://doi.org/10.1093/cid/ciaa201>.
- Kermack, W.O., McKendrick, A.G., 1927. A contribution to the mathematical theory of epidemics. *Proc. R. Soc. London Ser. A* 115, 700–721.
- Ke, R., Zitzmann, C., Ribeiro, R.M., Perelson, A.S., 2020. Kinetics of SARS-CoV-2 infection in the human upper and lower respiratory tracts and their relationship with infectiousness. *MedRxiv*. 2020.09.25.20201772. (<http://medrxiv.org/content/early/2020/09/27/2020.09.25.20201772.abstract>).
- Kissler, S.M., Tedijanto, C., Goldstein, E., Grad, Y.H., Lipsitch, M., 2020. Projecting the transmission dynamics of SARS-CoV-2 through the postpandemic period. *Science* 5793, 1–13.
- Kucirka, L.M., Lauer, S.A., Laeyendecker, O., Boon, D., Lessler, J., 2020. Variation in false-negative rate of reverse transcriptase polymerase chain reaction-based SARS-CoV-2 tests by time since exposure. *Ann. Intern. Med.* <https://doi.org/10.7326/m20-1495>.
- Larremore, D.B., Wilder, B., Lester, E., Shehata, S., Burke, J.M., Hay, J.A., Tambe, M., Mina, M.J., 2021. Test sensitivity is secondary to frequency and turnaround time for COVID-19 surveillance. *Sci. Adv.* 7, eabd5393.
- Lau, M.S.Y., Grenfell, B., Thomas, M., Bryan, M., Nelson, K., Lopman, B., 2020. Characterizing superspreading events and age-specific infectiousness of SARS-CoV-2 transmission in Georgia, USA. *Proc. Natl. Acad. Sci. USA* 117, 22430–22435. doi:10.1073/pnas.2011802117.
- Laxminarayan, R., Wahl, B., Dudala, S.R., Gopal, K., Mohan, C., Neelima, S., Reddy, K.S. J., Radhakrishnan, J., Lewnard, J.A., 2020. Epidemiology and transmission dynamics of COVID-19 in two Indian states. *Science* 28, eabd7672. (<http://journals.sagepub.com/doi/10.1177/1120700020921110%0Ahttps://doi.org/10.1016/j.reuma.2018.06.001%0Ahttps://doi.org/10.1016/j.arth.2018.03.044%0Ahttps://reader.elsevier.com/reader/sd/pii/S1063458420300078?token=C039B8B13922A2079230DC9AF11A333E295FCD8>).
- Liu, Y., Eggo, R.M., Kucharski, A.J., 2020. Secondary attack rate and superspreading events for SARS-CoV-2. *Lancet* 395, e47. [https://doi.org/10.1016/S0140-6736\(20\)30462-1](https://doi.org/10.1016/S0140-6736(20)30462-1).
- Liu, Y., Rocklöv, J., 2021. The reproductive number of the Delta variant of SARS-CoV-2 is far higher compared to the ancestral SARS-CoV-2 virus. *J. Travel Med.* 3, 584–586. <https://doi.org/10.46234/ccdcw2021.148>.
- Meyerson, N.R., Yang, Q., Clark, S.K., Paige, C.L., Fattor, W.T., Gilchrist, A.R., Barbachano-Guerrero, A., Sawyer, S.L., 2020. A community-deployable SARS-CoV-2 screening test using raw saliva with 45 min sample-to-results turnaround. *MedRxiv*. 2020.07.16.20150250. doi:10.1101/2020.07.16.20150250.
- Meyer, R., Madrigal, A.C., 2020. The Plan That Could Give Us Our Lives Back, *Atl.*
- Mizumoto, K., Kagaya, K., Zarebski, A., Chowell, G., 2020. Estimating the asymptomatic proportion of coronavirus disease 2019 (COVID-19) cases on board the Diamond Princess cruise ship, Yokohama, Japan, 2020. *Eurosurveillance* 25, 1–5. <https://doi.org/10.2807/1560-7917.ES.2020.25.10.2000180>.
- Nielsen, B.F., Sneppen, K., 2020. COVID-19 superspreading suggests mitigation by social network modulation. *MedRxiv*. 2020.09.15.20195008. (<http://medrxiv.org/content/early/2020/10/04/2020.09.15.20195008.abstract>).
- Nietzel, M.T., 2020. As Covid-19 Lingers On, Universities Are Adjusting Their Spring Semester Plans, Often Eliminating Spring Break, *Forbes*.
- Nishiura, H., Kobayashi, T., Miyama, T., Suzuki, A., Imai, N., Hayashi, K., Kinoshita, R., Yang, Y., Yuan, B., Akhmetzhanov, A.R., Linton, N.M., 2020. Estimation of the asymptomatic ratio of novel coronavirus infections (COVID-19). *Int. J. Infect. Dis.* 94, 154–155. <https://doi.org/10.1016/j.ijid.2020.03.020>.
- Nowak, M.A., May, R.M., 2000. *Virus Dynamics: Mathematical Principles of Immunology and Virology*. Oxford University Press, Oxford, UK.
- Oran, D.P., Topol, E.J., 2020. Prevalence of asymptomatic SARS-CoV-2 infection: a narrative review. *Ann. Intern. Med.* 173, 362–367. <https://doi.org/10.7326/M20-3012>.
- Paltiel, A.D., Zheng, A., Walensky, R.P., 2020. Assessment of SARS-CoV-2 screening strategies to permit the safe reopening of college campuses in the United States. *JAMA Netw. Open* 3, e2016818. <https://doi.org/10.1001/jamanetworkopen.2020.16818>.
- Peak, C.M., Kahn, R., Grad, Y.H., Childs, L.M., Li, R., Lipsitch, M., Buckee, C.O., 2020. Individual quarantine versus active monitoring of contacts for the mitigation of COVID-19: a modelling study. *Lancet Infect. Dis.* 3099 <https://doi.org/10.1016/2020.03.05.20031088>.
- Perelson, A.S., 2002. Modelling viral and immune system dynamics. *Nat. Rev. Immunol.* 2, 28–36. <https://doi.org/10.1038/nri700>.
- Petersen, E., Koopmans, M., Go, U., Hamer, D.H., Petrosillo, N., Castelli, F., Storgaard, M., Al Khalili, S., Simonsen, L., 2020. Comparing SARS-CoV-2 with SARS-CoV and influenza pandemics. *Lancet Infect. Dis.* 20, e238–e244. [https://doi.org/10.1016/S1473-3099\(20\)30484-9](https://doi.org/10.1016/S1473-3099(20)30484-9).
- Polack, F.P., Thomas, S.J., Kitchin, N., Absalon, J., Gurtman, A., Lockhart, S., Perez, J.L., Pérez Marc, G., Moreira, E.D., Zerbini, C., Bailey, R., Swanson, K.A., Roychoudhury, S., Koury, K., Li, P., Kalina, W.V., Cooper, D., Frenck, R.W., Hammitt, L.L., Túreci, Ö., Nell, H., Schaefer, A., Ünal, S., Tresnan, D.B., Mather, S., Dormitzer, P.R., Şahin, U., Jansen, K.U., Gruber, W.C., 2020. Safety and efficacy of the BNT162b2 mRNA Covid-19 vaccine. *N. Engl. J. Med.* 383, 2603–2615. <https://doi.org/10.1056/nejmoa2034577>.
- Poletti, P., Tirani, M., Cereda, D., Trentini, F., Guzzetta, G., Sabatino, G., Marziano, V., Castorino, A., Grosso, F., Del Castillo, G., Piccarreta, R., A.L.C.–19 T. Force, Andreassi, A., Melegaro, A., Gramegna, M., Ajelli, M., Merler, S., 2020. Probability of symptoms and critical disease after SARS-CoV-2 infection. *ArXiv*. (<http://arxiv.org/abs/2006.08471>).
- Quicke, K., Gallichotte, E., Sexton, N., Young, M., Janich, A., Gahm, G., Carlton, E.J., Ehrhart, N., Ebel, G.D., 2020. Longitudinal surveillance for SARS-CoV-2 RNA among asymptomatic staff in five Colorado skilled nursing facilities: epidemiologic, virologic and sequence analysis. *MedRxiv*. <https://doi.org/10.1101/2020.06.08.20125989v1>.
- R. of the U. of California, 2021. UC issues final COVID-19 vaccination policy, Ucnct. (<https://ucnet.universityofcalifornia.edu/news/2021/07/ucs-covid-19-vaccine-policy.html>).
- Richtel, M., 2020. Looking to Reopen, Colleges Become Labs for Coronavirus Tests and Tracking Apps, *New York Times*.
- de Rio, C., Malani, P.N., Omer, S.B., 2021. Confronting the Delta variant of SARS-CoV-2, summer 2021. *J. Am. Med. Assoc.* 385, 1244–1246. <https://doi.org/10.1056/nejmc2111462>.
- Saad-Roy, C.M., Wagner, C.E., Baker, R.E., Morris, S.E., Farrar, J.J., Graham, A.L., Levin, S.A., Mina, M.J., Metcalf, C.J.E., Grenfell, B.T., 2020. Immune life history, vaccination, and the dynamics of SARS-CoV-2 over the next 5 years. *Science* 21, 1–9. <https://doi.org/10.1126/science.1210768>.
- Schwab, J., Balzer, L.B., Geng, E., Peng, J., Petersen, M.L., n.d. Local Epidemic Modeling for Management and Action, (<https://localepi.github.io/LEMMA/>).
- La Scola, B., Le Bideau, M., Andreani, J., Hoang, V.T., Grimaldi, C., Colson, P., Gautret, P., Raoult, D., 2020. Viral RNA load as determined by cell culture as a management tool for discharge of SARS-CoV-2 patients from infectious disease wards. *Eur. J. Clin. Microbiol. Infect. Dis.* 39, 1059–1061. <https://doi.org/10.1007/s10096-020-03913-9>.
- Thomas, A., O'Leary, B., 2021. Here's a List of Colleges That Require Students or Employees to Be Vaccinated Against Covid-19, *Chronical High. Educ.* (https://www.chronicle.com/blogs/live-coronavirus-updates/heres-a-list-of-colleges-that-will-req-uire-students-to-be-vaccinated-against-covid-19?bc_nonce=7dz1p1qvlwvwnq51dsjs6jm&cid=reg_wall_signup).
- Treibel, T.A., Manisty, C., Burton, M., McKnight, A., Lambourne, J., Augusto, J.B., Couto-Parada, X., Cutino-Moguel, T., Noursadeghi, M., Moon, J.C., 2020. COVID-19: PCR screening of asymptomatic health-care workers at London hospital. *Lancet*. 395, 1608–1610. [https://doi.org/10.1016/S0140-6736\(20\)31100-4](https://doi.org/10.1016/S0140-6736(20)31100-4).
- U.B. Public Affairs, 2020. Social gatherings produce increase in student COVID-19 cases, *Berkeley News*.
- U.S.D. Health, CA Notify, 2020. (<https://canotify.ca.gov/>) (accessed December 21, 2020).
- UC Berkeley COVID-19 Dashboard, 2020. (https://coronavirus.berkeley.edu/dashboard/?utm_source=Response+and+Recovery&utm_campaign=5247da06c4-Response_Recovery_2020_10_09&utm_medium=email&utm_term=0_940930e328-5247da06c4-389116456) (accessed October 1, 2021).
- University of Alabama System COVID-19 Dashboard, n.d.
- Vaziri, A., Asimov, N., 2021. Stanford among first universities requiring weekly coronavirus testing - even for vaccinated students, *San Fr. Chron.*
- Vogels, C.B.F., Brito, A.F., Wyllie, A.L., Fauver, J.R., Ott, I.M., Kalinich, C.C., Petrone, M. E., Casanovas-Massana, A., Catherine Muenker, M., Moore, A.J., Klein, J., Lu, P., Lu-Culligan, A., Jiang, X., Kim, D.J., Kudo, E., Mao, T., Moriyama, M., Oh, J.E., Park, A., Silva, J., Song, E., Takahashi, T., Taura, M., Tokuyama, M., Venkataraman, A., El Weizman, O., Wong, P., Yang, Y., Cheemarla, N.R., White, E.B., Lapidus, S., Earnest, R., Geng, B., Vijayakumar, P., Odio, C., Fournier, J., Bermejo, S., Farhadian, S., Dela Cruz, C.S., Iwasaki, A., Ko, A.I., Landry, M.L., Foxman, E.F., Grubaugh, N.D., 2020. Analytical sensitivity and efficiency comparisons of SARS-CoV-2 RT-qPCR primer-probe sets. *Nat. Microbiol.* <https://doi.org/10.1038/s41564-020-0761-6>.
- WHO, 2020. Coronavirus disease (COVID-2019) situation reports, (<https://www.who.int/emergencies/diseases/novel-coronavirus-2019/situation-reports>) (accessed June 30, 2020).
- Wölfel, R., Corman, V.M., Guggemos, W., Seilmaier, M., Zange, S., Müller, M.A., Niemeyer, D., Jones, T.C., Vollmar, P., Rothe, C., Hoelscher, M., Bleicker, T., Brünink, S., Schneider, J., Ehmann, R., Zwirgmaier, K., Drosten, C., Wendtner, C., 2020. Virological assessment of hospitalized patients with COVID-2019. *Nature* 581, 465–469. <https://doi.org/10.1038/s41586-020-2196-x>.
- Wu, K.J., 2020. 'It's Like Groundhog Day': Coronavirus Testing Labs Again Lack Key Supplies, *New York Times*.